Supporting Information

Zhou et al. 10.1073/pnas.1105254108

Materials and Methods

LNA-Anti-miRs, Pre-miR Precursors, siRNAs, and miRNA Expressing Adenoviruses. LNA-anti-miRs for miR-23a/b, miR-27a/b, or scramble controls for in vitro and in vivo studies were synthesized from Exiqon. LNA-anti-miR-27a/b sequence for in vitro use is: 5′-GAACTTAGCCACTGTGAA-3′ (product no. 500150, batch no. 604052). LNA-anti-miR-23a/b sequence for in vitro use is: 5′-AATCCCTGGCAATGTGAT-3′ (product no. 500150, batch no. 604053). LNA-scramble control sequence for in vitro use is: 5′-GTGTAACACGTCTATACGCCCA-3′ (product no. 199004–00, batch no. 205157). LNA-anti-miR-27a/b sequence for in vivo use is: 5′-ACTTAGCCACTGTGA-3′ (product no. 500150, batch no. 603226). LNA-anti-miR-23a/b sequence for in vivo use is: 5′-TCCCTGGCAATGTGA-3′ (product no. 500150, batch no. 603227). LNA-scramble control sequence for in vivo use is: 5′-ACGTCTATACGCCCA-3′ (product no. 500150, batch no. 603228). LNA-anti-miRs were typically transfected at a final concentration of 50 nM using Lipofectamine 2000 (Invitrogen) as transfection reagent. SiRNAs for SPROUTY2 were synthesized from Dharmacon. The target sequence for SPROUTY2 siRNA is 5′-GCAGGUACACGUCUUGUCU-3′. Ambion pre-miR miRNA precursor of hsa-miR-23b, hsa-miR-27b, or negative control was synthesized from Applied Biosystems. Adenovirus expressing miR-23b, miR-27b, or lacZ was generated from mouse genomic DNA encoding miR-23b or -27 as described (1).

Cell Culture, Cell Proliferation, Scratch-Wound, in Vitro Matrigel, and Aortic Ring Sprouting Assays. HUVEC (ATCC) cells were grown in EC growth medium (Lonza). SEMA6A recombinant protein was obtained from R&D. For VEGF treatment, HUVECs were starved with EC basal medium-2 with 0.1% FBS for 24 h and then treated with VEGF (20 ng/mL) for the indicated periods of time. For LPS treatment, HUVECs were treated with LPS (100 ng/mL) for the indicated periods of time without starvation. Adenovirus infection, siRNA, pre-miR miRNA precursor, or LNA-anti-miR transfection in cell culture and aortic ring culture was performed as described (2). EC cell proliferation and scratch-wound assays were performed using HUVEC cells as described (1, 3). For cellular proliferation assay, about 2×10^3 transfected HUVECs were seeded in 24-well plates. After starvation with 0.1% serum for overnight, the cells were stimulated with 20 ng/mL VEGF-A for 20 h and then subjected to BrDU labeling for 4 h. DNA synthesis as determined by BrDU incorporation was quantified using a commercial ELISA kit from Roche according to the manufacturer's instructions. For scratch wound assay, scratch-wound was made using a 200-μL pipette tip in LNA anti-miR–transfected HUVEC monolayer before VEGF (20 ng/mL) stimulation. Then 1 μM of 5-fluouracil (Sigma) was added to the cell right after scratch wound to block cell proliferation. Post-scratch EC migration was scored at 14 h after wound scratch. In vitro angiogenesis assays were performed as described (4). Briefly, 3 d after LNA anti-miR transfection with Liptofectamine Plus reagent (Invitrogen), cells were harvested for either RNA analysis or in vitro angiogenesis. Matrigel was purchased from Chemicon, and the assays were performed according to manufacturer's manual. Briefly, HUVECs were transfected with anti-miR or scramble control using lipofectamine 2000 and cultured for 48 h, serum starved overnight, then trypsinized and used for Matrigel assay. Quantification of branch points per field (20×) was done on six fields and six sample repeats.

RNA, Western Blot Analysis, and Reporter Assay. Total RNA was isolated from mouse tissues or cell lines using TRIzol reagent (Invitrogen). Northern blots to detect microRNAs were performed as described (2). Real-time RT-PCR using Sybergreen probes was performed using 1 μg of RNA as a template with random hexamer primers to generate cDNA. miRNA real-time RT-PCR was performed using miRCURY LNA Universal microRNA RT-PCR system (Exiqon). For PCR and cloning of miR-23~27~24 pri-miRNAs, Race-Ready cDNA from mouse embryos (Ambion) was used. Sequences of PCR primers for SPROUTY2, SPROUTY2 (miR-23m), SPROUTY2 (miR-27m), SEMA6D 3′UTRs, and mouse miR-23a~27a~24–2 and miR-23b~27b~24–1 pri-miRNA are listed as follows:

i) hSPROUTY2-3′UTR (SacI): 5′-atcg gagctc AGCAACACAGACACTCCTAGGCA-3′
ii) hSPROUTY2-3′UTR (HindIII): 5′-atcg aagctt GCATCTGTAACCCCTCATTTGCAGC-3′
iii) hSPROUTY2 (miR-27mut) up: 5′-caataatatttgcacagactccaaacaagttgtgc-3′
iv) hSPROUTY2 (miR-27mut) dn: 5′-gcacaacttgtttggagtctgtgcaaatattattg-3′
v) hSPROUTY2 (miR-23mut1) up: 5′-gtacattcggaagccgacagatcaatcagtatg-3′
vi) hSPROUTY2 (miR-23mut1) dn: 5′-catactgattgatctgtcggcttccgaatgtac-3′
vii) hSPROUTY2 (miR-23mut2)dn: 5′-atcg aagctt gcatctgtaaccccctcatttgcagcaactcgag tcgcctcataa aaggggc-3′
viii) hSEMA6D-3′UTR (SacI): 5′- atcggagctcCCCACTGGGGCGAAGGTGGA-3′
ix) hSEMA6D-3′UTR (HindIII): 5′-atcgaagcttAGGGTTGCGCATCATCAGCCGT-3′
x) mPri-miR-23a~27a~24–2 (up): 5′- CTGGTGCATTCGGAAACCTTGTGT -3′
xi) mPri-miR-23a~27a~24–2 (dn): 5′- ATTGGAGCATTCTTGCTTGCCTGC -3′
xii) mPri-miR-23b~27b~24–1 (up): 5′- ATGAAAGAGACGCACTAGCCCACA -3′
xiii) mPri-miR-23b~27b~24–1 (dn): 5′- TTGGGTTCCTGGCATGCTGATTTG -3′

For Western blot analysis, protein lysates were resolved by SDS/PAGE and blotted using standard procedures. Antibodies used were as follows: ERK1/2 (Cell Signaling), phospho-ERK1/2 (Cell Signaling), phospho-AKT (Cell Signaling), SPROUTY2 (Abcam), SEMA6A (R&D), SEMA6D (R&D), and GAPDH (Abcam) as loading control. Band intensity was quantified using National Institutes of Health ImageJ software and normalized to correspondent GAPDH signal. For reporter assay, the 3′UTR of SPROUTY2 or SEMA6D was inserted into the pMIR-REPORT vector (Ambion). SEMA6A 3′UTR construct was purchased from Genecopeia. SPROUTY2 3′UTRs with mutations in the region complementary to the miR-23 or miR-27 seed regions were generated by mutagenesis. Pre-miR miRNA precursors (ABI) were cotransfected with the UTR plasmids indicated into COS-7 cells. Reporter assays were performed as described (5).

Neonatal Retinal Injection and Postnatal Retinal Angiogenesis. In vivo injection in the mouse retina was performed primarily as described (6). Briefly, 1 μL of 5 mg/mL solution of LNA-anti-miR23 and miR-27 or LNA-scramble control was unilaterally injected intravitreously into the retina of P2 mice in the ICR background. Mice were allowed to develop for RNA, protein isolation,

and histological analyses at P6. Visualization of the vasculature was performed by Alexa-594 conjugated isolectin B4 (Molecular Probes) or ICAM-2 staining of retinal flat mounts. Quantification of vessel density was performed using National Institutes of Health ImageJ software. The radial length of the vascular network was calculated by measuring the distance from the optic disk to the periphery of the vascular plexus. Student *t* tests were used to determine statistical significance between groups.

Laser-Induced CNV. Laser photocoagulation was induced in 6- to 8-wk-old male C57BL/6J mice as described (7). Briefly, the pupils of anesthetized animals were dilated with 1% tropicamide (Alcon Laboratories). Three 532-nm diode laser spots (140 mW, 100 ms, 100 μm; OcuLight GL Photocoagulator, Iridex) were applied to each fundus of adult mice using a coverslip as a contact lens. Six laser spots were applied when the samples were used for RNA isolation. Formation of a bubble at the time of laser application indicates rupture of Bruch's membrane and successful laser injury. Animals were intravitreously injected with 1 μL of 5 mg/mL solution of LNA-anti-miR23/27, LNA-scramble or PBS injection control after laser photocoagulation. A secondary injection was adopted on the next day to ensure maximal knockdown of miR-23/27. The retina/choroid/sclera complexes from the treated eyes were collected 7 d after laser injury for fluorescein angiography, RNA, and protein analyses. At 14 d after laser injury, the eyes were fixed in 4% paraformaldehyde for 30 min at room temperature. The retina/choroid/sclera complexes were then dissected and fixed for frozen section or flatmount staining. For flatmount staining, the samples were postfixed for 1 h, incubated with blocking buffer (PBS with 0.5% Triton X-100 and 5% goat serum), and stained with ICAM-2 antibody at 4 °C overnight. After washing and secondary antibody staining, the samples were flat mounted on glass slides. Images of CNV were captured using a Leica SP2 multiphoton Laser Scanning confocal microscope, and CNV volume was quantified using National Institutes of Health ImageJ software. Student *t* tests were used to determine statistical significance between groups.

1. Wang S, et al. (2008) Control of endothelial cell proliferation and migration by VEGF signaling to histone deacetylase 7. *Proc Natl Acad Sci USA* 105:7738–7743.
2. Wang S, et al. (2008) The endothelial-specific microRNA miR-126 governs vascular integrity and angiogenesis. *Dev Cell* 15:261–271.
3. Lee KS, et al. (2006) Troglitazone inhibits endothelial cell proliferation through suppression of casein kinase 2 activity. *Biochem Biophys Res Commun* 346:83–88.
4. Chang S, et al. (2006) Histone deacetylase 7 maintains vascular integrity by repressing matrix metalloproteinase 10. *Cell* 126:321–334.
5. Chang S, Bezprozvannaya S, Li S, Olson EN (2005) An expression screen reveals modulators of class II histone deacetylase phosphorylation. *Proc Natl Acad Sci USA* 102:8120–8125.
6. Matsuda T, Cepko CL (2004) Electroporation and RNA interference in the rodent retina in vivo and in vitro. *Proc Natl Acad Sci USA* 101:16–22.
7. Tobe T, et al. (1998) Targeted disruption of the FGF2 gene does not prevent choroidal neovascularization in a murine model. *Am J Pathol* 153:1641–1646.

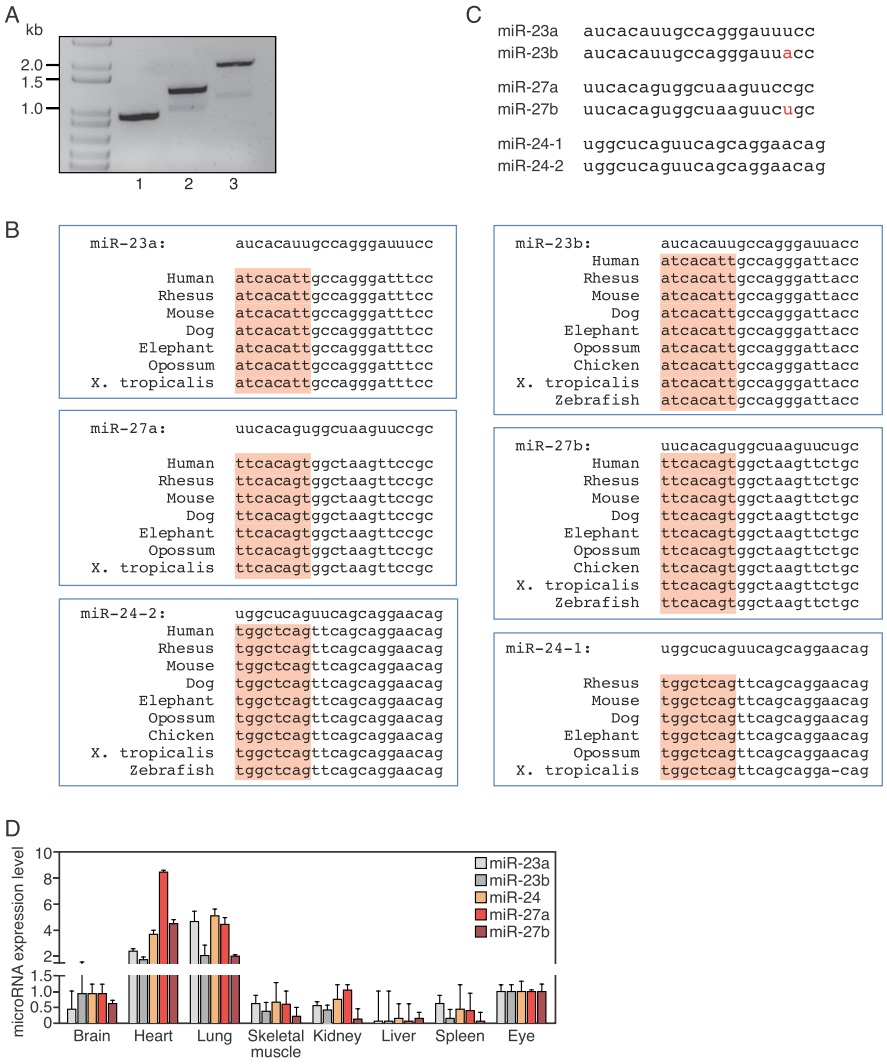

Fig. S1. (*A*) Expression of pri-miRNA of mouse miR-23~27~24 clusters as examined by RT-PCR using Race Ready cDNA from mouse embryos (Ambion). Lane 1 is the PCR product using primer A and B shown in Fig. 1*A*. Lane 2 is the PCR product using Primer C and D, and lane 3 is the PCR product using Primer C and E shown in Fig. 1*A*. (*B*) Evolutionary conservation of miR-23~27~24 clusters in vertebrate species using Human Blat (http://genome.ucsc.edu/cgi-bin/hgBlat?command=start). The seed regions are highlighted. (*C*) Sequences of mature miRNAs of mouse miR-23~27~24 clusters. The differences between the sequence of miR-23a and miR-23b, or miR-27a and miR-27b, are indicated in red. (*D*) Expression of miR-23~27~24 cluster members in different tissues as detected by real-time PCR using LNA-modified miRNA probes. U6 served as a normalization control.

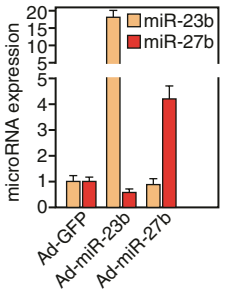

Fig. S2. Efficient overexpression of miR-23 or miR-27 in cultured aortic rings by adenovirus expressing miR-23b or miR-27b, as shown by real-time PCR with LNA-modified miRNA primers.

A

Pathways regulated by miR-23 and miR-27 predicted by DIANA Lab (DIANA-mirPath)				
	KEGG Pathway (Rank)	Gene Names	Found genes	-ln(p-value) (p-value)
miR-23 OR miR-27	Axon guidance (1)	EFNB2, SRGAP3, SEMA6A, NCK2, SLIT1, CXCL12, ITGB1, LIMK1, LIMK2, EFNA3, EPHB2, MET, SEMA6D, SRGAP2, KRAS, PAK3, FYN, CFL2, EPHA7, SEMA4C, UNC5D, CDC42, PAK2, PAK6, ROBO2, SEMA3B, SEMA4F	27	12.39 (0.00018)
	MAPK signaling pathway (8)	MAP4K3, MAP4K4, PRKY, PDGFRA, EVI1, TGFBR1, MAP3K4, MAP3K1, MAPKAPK3, KRAS, CACNB2, MEF2C, MKNK2, DUSP5, STK4, MAP2K4, SOS1, DUSP16, PRKX, MAP3K3, RPS6KA5, FGF1, CDC25B, CDC42, GRB2, PAK2, MAP2K7, RAP1B, NLK, NF1, TGFBR2, MAPK14, MAP3K12, RPS6KA3, MAP3K5, MAPK10, SPROUTY2	37	4.78 (0.013)
miR-23 AND miR-27	MAPK signaling pathway (1)	EVI1, CACNB2, MEF2C, DUSP5, SOS1, RPS6KA5, NLK, NF1, MAPK14, MAP3K12, SPROUTY2	11	14.54 ($4.2x10^{-5}$)
	Axon guidance (5)	MET, SEMA6A, SEMA6D, FYN, PAK6	5	3.85 (0.07)

B

Gene name	miRNA	Position	Site	3'UTR (sequence complementary to miRNA seeds highlighted in red)	Conservation (species#)
SPROUTY2	miR-23a/b	436-464	2 ; 8mer	5′...GGAGGAAUGUGAA...3′	11
		678-706	1 ; 7mer	5′...UAUGAGGAUGUGAU...3′	5
	miR-27a/b	360-388	1 ; 8mer	5′...AUUUGCAACUGUGAA...3′	13
SEMA6A	miR-23a/b	1832-1860	1 ; 6mer	5′...UCCCUGCUGUGAU...3′	7
	miR-27a/b	546-574	1 ; 8mer	5′...GCGCAAAUACUGUGAA...3′	11
		1250-1278	1 ; 7mer	5′...GGGUUACAUCUGUGAA...3′	8
		1110-1128	1 ; 7mer	5′...UCUGACUUUCUGUGAA...3′	5
		2388-2416	1 ; 7mer	5′...GUUCACAUCCUGUGAA...3′	3
SEMA6D	miR-23a/b	1590-1618	2 ; 8mer	5′...CCCAUUAAAUGUGAA...3′	11
		2748-2776	2 ; 8mer	5′...CAGUGAUAAUGUGAA...3′	7
		2777-2805	2 ; 8mer	5′...CCUGGGUAAUGUGAC...3′	5
		3359-3387	2 ; 8mer	5′...AGUUUGUAAUGUGAG...3′	9
		3051-3079	2 ; 8mer	5′...UAUACAGAAUGUGAA...3′	1
	miR-27a/b	2158-2186	1 ; 10mer	5′...UCCUGUCCACUGUGAA...3′	9
		1526-1554	1 ; 7mer	5′...CAGAAGAAUCUGUGAA...3′	2

Fig. S3. (*A*) Pathways regulated by miR-23 and/or miR-27 predicted using DIANA-mirPath from DIANALab. (*B*) A table showing several miRs-23/27 target genes with potential roles in angiogenesis. These genes are predicted by DIANA-microT v3.0 and/or TargetScan algorithms to be miR-23 and miR-27 targets. The sequences in the target genes complementary to the miRNA seed regions are shown in red. The number of species in which the target sites are conserved is shown.

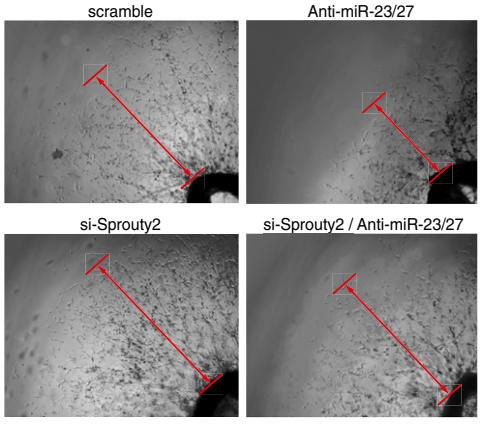

Fig. S4. Representative pictures of ex vivo aortic ring assays 6 d after anti-miR-23/27 and/or Sprouty2 siRNA transfection in cultured aortic rings. Sprouting of the aortic ring cells is indicated by the red lines.

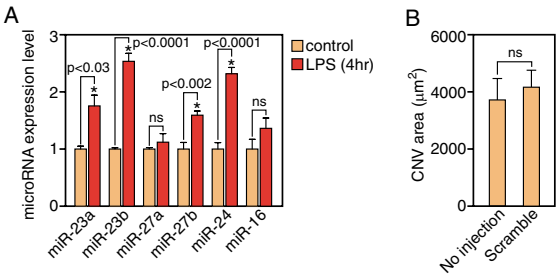

Fig. S5. (*A*) Expression of miR-23~27~24 cluster members in HUVECs induced by LPS, as detected using LNA-modified miRNA PCR primers. U6 served as a normalization control. (*B*) Quantification of CNV area from ICAM-2 staining of the choroid l flatmounts measured from control-injected retinas and no-injection control retinas 14 d after laser injury. ns, not significant.